RNA interference machinery influences the nuclear organization of a chromatin insulator

Elissa P Lei & Victor G Corces

RNA interference (RNAi) is a conserved silencing mechanism that can act through alteration of chromatin structure. Chromatin insulators promote higher-order nuclear organization, thereby establishing DNA domains subject to distinct transcriptional controls. We present evidence for a functional relationship between RNAi and the *gypsy* insulator of *D. melanogaster*. Insulator activity is decreased when Argonaute genes required for RNAi are mutated, and insulator function is improved when the levels of the Rm62 helicase, involved in double-stranded RNA (dsRNA)-mediated silencing and heterochromatin formation, are reduced. Rm62 interacts physically with the DNA-binding insulator protein CP190 in an RNA-dependent manner. Finally, reduction of Rm62 levels results in marked nuclear reorganization of a compromised insulator. These results suggest that the RNAi machinery acts as a modulator of nuclear architecture capable of effecting global changes in gene expression.

RNAi is a highly conserved cellular mechanism to reduce mRNA usage in a sequence-specific manner. In addition, RNAi can control gene expression by altering the state of chromatin. For example, RNAi is required to establish centromeric heterochromatin in *S. pombe*[1] and *D. melanogaster*[2]. RNAi also has a role in the nuclear positioning of silent chromatin, as *S. pombe* RNAi mutants show telomere clustering defects[3], and Polycomb-dependent pairing-sensitive silencing of transgenes is reduced in *D. melanogaster* RNAi mutants[4].

Chromatin insulators participate in the establishment and maintenance of distinct transcriptional domains. Two functional properties are the abilities to interfere with promoter-enhancer interactions and shield transgenes from position effects caused by surrounding chromatin. The *gypsy* insulator sequence harbors binding sites for the DNA-binding protein Suppressor of Hairy wing (Su(Hw))[5]. Two additional protein components are the DNA-binding Centrosomal protein 190 (CP190) and Modifier of mdg4 2.2 (Mod(mdg4)2.2)[6,7]. Existing as a complex, insulator proteins concentrate in nuclear foci termed insulator bodies, and insulator activity correlates with the ability to form these higher-order structures[6,8,9]. Proper localization of insulator bodies requires an intact nuclear matrix scaffold, and in particular, the presence of lamin as well as RNA[9,10]. Chromatin
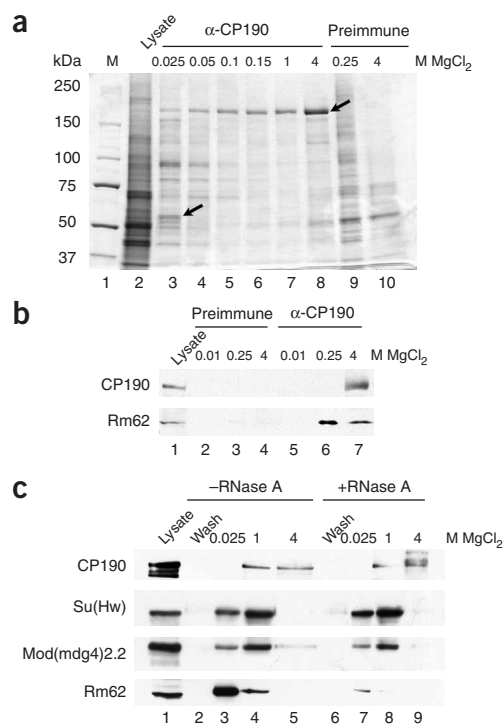

Figure 1 The insulator protein CP190 interacts with the RNA helicase Rm62 in an RNA-dependent manner. (**a**) Immunoaffinity purification of CP190-associated proteins. Embryonic nuclear extracts (lane 2) were bound to an α-CP190 column (lanes 3–8) or control preimmune column (lanes 9–10), and bound proteins were eluted sequentially with increasing MgCl$_2$ concentrations. Eluates were electrophoresed by SDS-PAGE and stained with Coomassie blue. Proteins associated uniquely with the α-CP190 column were identified by MALDI-TOF mass spectrometry. Arrows mark proteins that correspond to CP190 (lane 8) and Rm62 (lane 3). (**b**) Protein blotting of control preimmune (lanes 2–4) and α-CP190 column (lanes 5–7) immunoaffinity purifications to verify the presence of CP190 and Rm62 in α-CP190 eluates. (**c**) α-CP190 immunoaffinity purifications performed in the absence (lanes 2–5) or presence (lanes 6–9) of RNase A. Protein blotting of CP190, Su(Hw), Mod(mdg4)2.2, and Rm62.

Department of Biology, Johns Hopkins University, Baltimore, Maryland, 21218, USA. Correspondence should be addressed to V.G.C. (corces@jhu.edu).
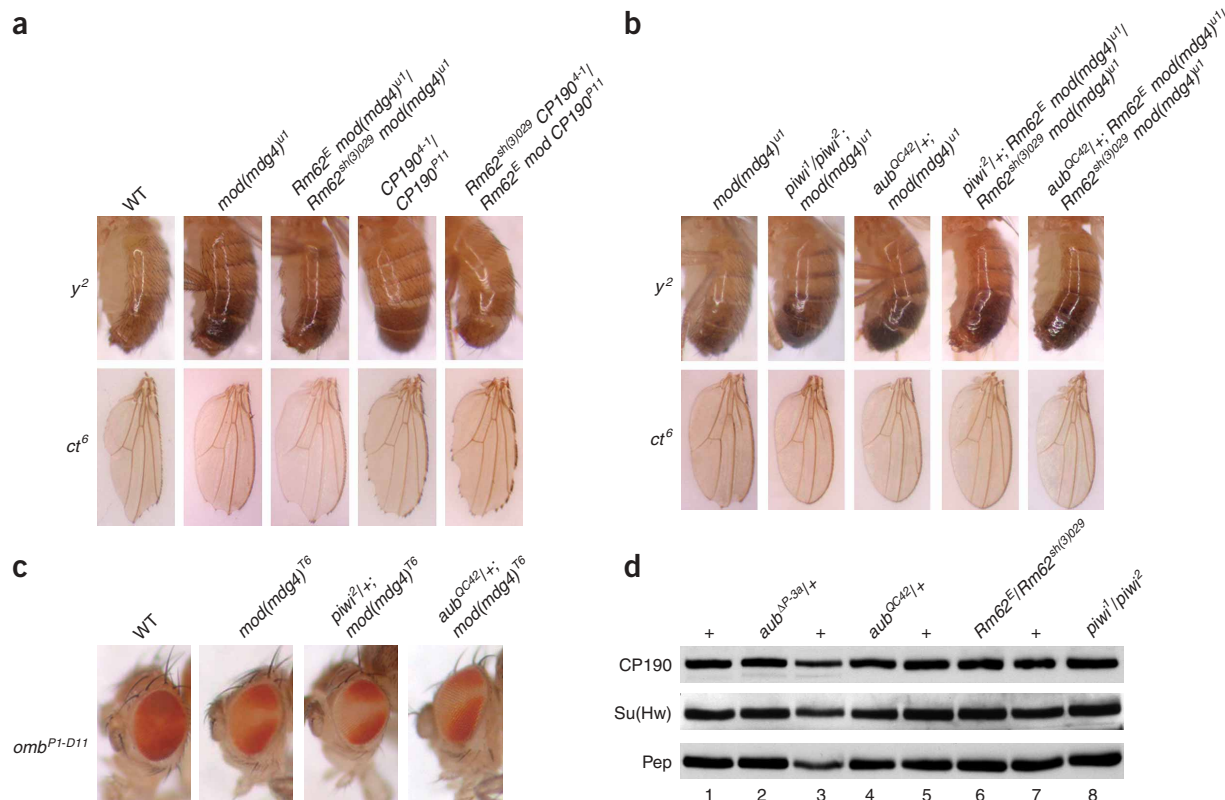
a

b

c

d

Figure 2 Mutations in genes required for RNAi affect *gypsy* insulator function. (**a**) Black pigmentation as a result of y^2 expression in the abdomen (top row) and expression of ct^6 in the wing (bottom row) of wild-type, $mod(mdg4)^{u1}$, $Rm62^E mod(mdg4)^{u1}/Rm62^{sh(3)029}mod(mdg4)^{u1}$, $CP190^{4-1}/CP190^{P11}$ and $Rm62^{sh(3)029}CP190^{4-1}/Rm62^E CP190^{P11}$ flies. Flies were examined for y^2 expression 2 d after eclosion. (**b**) Expression of y^2 in the abdomen (top row) and expression of ct^6 in the wing (bottom row) of $mod(mdg4)^{u1}$, $piwi^1/piwi^2$; $mod(mdg4)^{u1}$, $aub^{QC42}/+$; $mod(mdg4)^{u1}$, $piwi^2/+$; $Rm62^E mod(mdg4)^{u1}/Rm62^{sh(3)029}mod(mdg4)^{u1}$ and $aub^{QC42}/+$; $Rm62^E mod(mdg4)^{u1}/Rm62^{sh(3)029}mod(mdg4)^{u1}$ flies. Flies were examined for y^2 expression 1 d after eclosion. (**c**) Expression of *white* owing to the omb^{P1-D11} in the eye of wild-type, $mod(mdg4)^{T6}$, $piwi^2/+$; $mod(mdg4)^{T6}$ and $aub^{QC42}/+$; $mod(mdg4)^{T6}$ flies. (**d**) Protein blotting of CP190, Su(Hw) and Pep in $mod(mdg4)^{u1}$ (lanes 1, 3, 5, 7), $aub^{4P-3a}/+$; $mod(mdg4)^{u1}$ (lane 2), $aub^{QC42}/+$; $mod(mdg4)^{u1}$ (lane 4), $Rm62^E mod(mdg4)^{u1}/Rm62^{sh(3)029}mod(mdg4)^{u1}$ (lane 6) and $piwi^1/piwi^2$; $mod(mdg4)^{u1}$ (lane 8) anterior larval extracts.

insulators such as *gypsy* and vertebrate CCCTC-binding factor (CTCF) have been proposed to act as attachment regions that bridge two or more DNA sequences, causing DNA looping and the creation of a distinct chromatin domain[8,11]. Here we present evidence that the RNAi machinery influences the higher-order nuclear organization of the *gypsy* insulator, thereby affecting its ability to control gene expression.

To identify previously unknown *gypsy* insulator–associated proteins, we purified insulator complexes by immunoaffinity purification.

We bound embryonic nuclear extracts to columns cross-linked to antibodies to CP190 (α-CP190) or preimmune sera and eluted with increasing amounts of $MgCl_2$. We identified proteins associated specifically with the α-CP190 column by mass spectrometry, confirming the presence of CP190 (**Fig. 1a**). We identified a copurifying 68-kDa protein in the 25 mM $MgCl_2$ elution as the DEAD-box putative RNA helicase Rm62 (also known as Dmp68) encoded by the essential gene *Rm62* (also known as *Lip*), which is required for
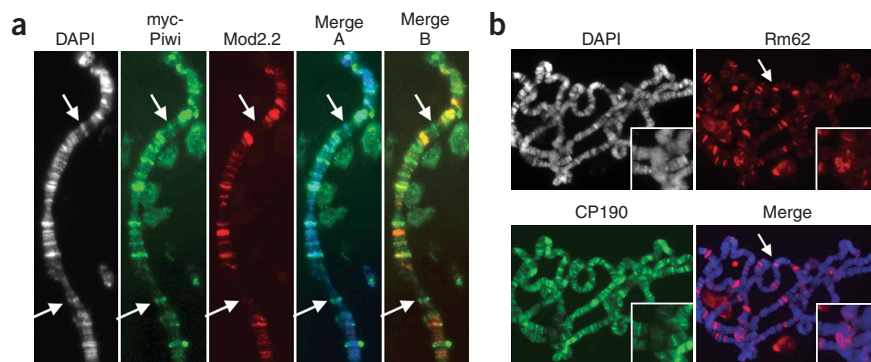
a

b

Figure 3 Localization of myc-Piwi and insulator proteins on polytene chromosomes. (**a**) α-myc and α-Mod(mdg4)2.2 staining of polytene chromosomes of otu^7/otu^{11} ovarian nurse cells expressing a *myc-piwi* transgene. Merges of DAPI with α-myc signal (merge A) and α-myc with α-Mod(mdg4)2.2 (merge B) are shown. Arrows point to two sites of DAPI and α-myc colocalization with little or no α-Mod(mdg4)2.2 staining. (**b**) α-Rm62 and α-CP190 staining of polytene chromosomes of the salivary gland. Insets show chromocenter at higher magnification. Merge of DAPI with α-Rm62 signal is shown at lower right; DAPI staining is shown at upper left. Arrow points to an ecdysone puff.
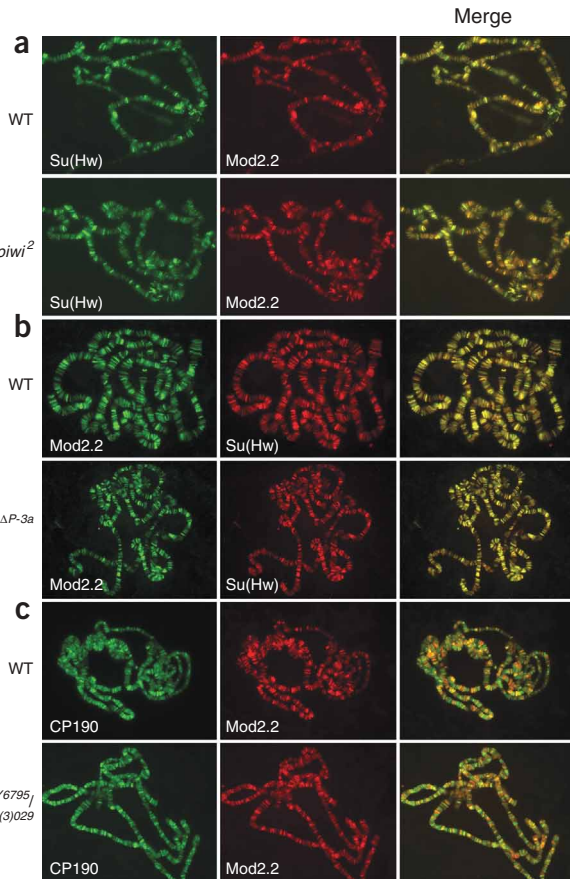
Figure 4 Localization of insulator proteins on polytene chromosomes of RNAi mutants. (**a**) Indirect immunofluorescence using α-Su(Hw) and α-Mod(mdg4)2.2 antibodies in wild-type (WT) larvae (upper row) and *piwi¹/piwi²* mutants (lower row). Merged images are shown at right. (**b**) α-Mod(mdg4)2.2 and α-Su(Hw) staining in wild-type larvae (upper row) and *aub^QC42* mutants (lower row). (**c**) α-CP190 and α-Mod(mdg4)2.2 staining in wild-type larvae (upper row) and *Rm62^EY6795/Rm62^sh(3)029* mutants (lower row).

levels of black pigmentation were visible in the abdomen owing to intermediate *y²* expression (**Fig. 2a**). In this genetic background, *ct⁶* is not fully expressed, resulting in a notched wing margin. Combination of *mod(mdg4)^u1* with a viable transheterozygous loss-of-function mutation in the gene that encodes Rm62, *Rm62^E/Rm62^sh(3)029*, resulted in decreased pigmentation and larger notches in the wing margin compared with *mod(mdg4)^u1* alone, indicating improvement of insulator activity (**Fig. 2a**). Like *mod(mdg4)^u1*, *CP190^4-1/CP190^P11* loss-of-function mutants caused by a nonsense mutation in one copy of *CP190* and deletion of the second copy showed reduced insulator activity. Combined mutation of *Rm62^E/Rm62^sh(3)029* and *CP190^4-1/CP190^P11* improved insulator function at *y²* but less so at *ct⁶* (**Fig. 2a**). These results suggest that wild-type Rm62 activity negatively affects insulator function *in vivo*.

In contrast to Rm62, Argonaute proteins exert a positive effect on insulator function. Mutations in two Argonaute genes required for RNAi-mediated heterochromatin formation, *piwi* and *aubergine²*, were tested for insulator activity. Recessive loss-of-function mutations in both genes cause defects in female sterility but not viability[17,18]. Compared with *mod (mdg4)^u1*, both *piwi¹/piwi²; mod(mdg4)^u1* and *aub^QC42/+; mod(mdg4)^u1* double mutants showed increased pigmentation and restoration to a round wing margin, indicating reduced insulator activity (**Fig. 2b**). We obtained similar results with *aub^ΔP-3a/+, piwi¹/+* and *piwi²/+* heterozygous mutants, and we also observed strong maternal effects of Argonaute mutations (data not shown). Additionally, heterozygous Argonaute mutations
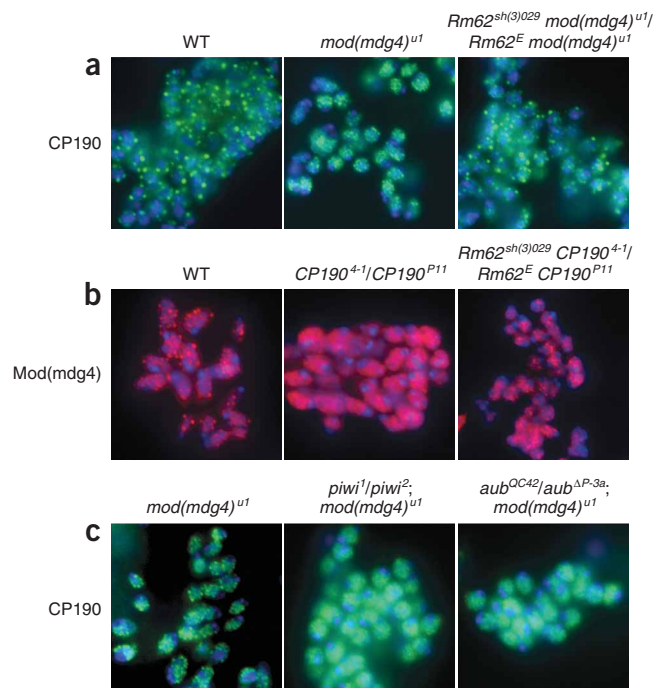
dsRNA-mediated silencing, heterochromatin formation and transposon silencing[12,13]. We verified the presence of CP190 and Rm62 in the purified complexes by protein blotting (**Fig. 1b**).

CP190 and Rm62 interact physically in an RNA-dependent manner. Given that Rm62 is a putative RNA-binding protein, we repeated the purifications in the presence or absence of RNase A. The amount of CP190 recovered was unchanged by the addition of RNase A, and interaction of CP190 with the insulator proteins Su(Hw) and Mod(mdg4)2.2 was unaffected (**Fig. 1c**). However, the amount of Rm62 copurifying with CP190 was reduced greatly when we added RNase A, indicating an RNA-dependent physical association.

We next tested whether mutation of the RNAi machinery alters insulator function. Insertion of the *gypsy* retrotransposon into *y²*, *ct⁶* and *omb^P1-D11* results in enhancer-specific gene expression defects dependent on insulator activity[14–16]. The insulator blocks enhancer-promoter communication of *y²* and *ct⁶*, resulting in decreased expression. In the sensitized *mod(mdg4)^u1* null mutant caused by insertion of a *stalker* retroelement, which has reduced insulator activity, moderate

Figure 5 Insulator body nuclear organization is altered in RNAi mutants. (**a**) Indirect immunofluorescence of larval diploid imaginal disc and brain cells using α-CP190 antibodies in wild-type (WT) larvae and *mod(mdg4)^u1* and *Rm62^sh(3)029mod(mdg4)^u1/Rm62^Emod(mdg4)^u1* mutants. (**b**) α-Mod(mdg4) staining in wild-type larvae and *CP190^4-1/CP190^P11* and *Rm62^sh(3)029CP190^4-1/Rm62^ECP190^P11* mutants. (**c**) α-CP190 staining in *mod(mdg4)^u1*, *piwi¹/piwi²; mod(mdg4)^u1* and *aub^QC42/aub^ΔP-3a; mod(mdg4)^u1* mutants. Merge of immunostaining (green or red) and DAPI staining (blue) is shown.
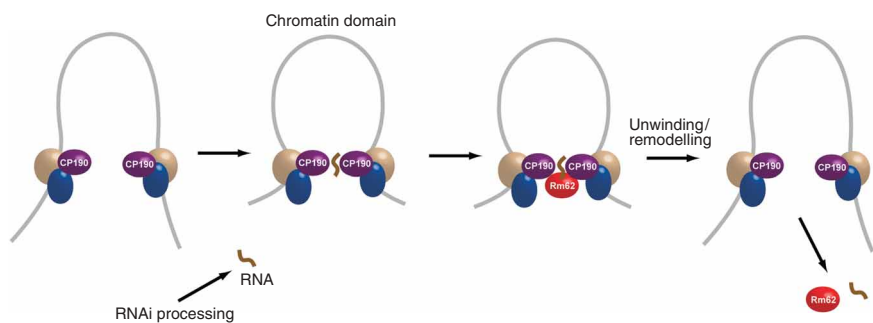
Figure 6 Model for how RNAi affects *gypsy* insulator chromatin domain formation. The *gypsy* insulator proteins Su(Hw) (beige), Mod(mdg4)2.2 (blue) and CP190 (purple) bind to insulator DNA sequences. RNAs processed by the RNAi machinery and possibly the RNAi machinery itself promotes higher-order insulator complex formation to produce an independent chromatin domain. Alternatively, RNAs may be required for the tethering of insulator complexes to the nuclear matrix. Recruited through physical contact with CP190 and RNA, Rm62 (red) unwinds or remodels protein/RNA complexes, thereby disassociating higher-order insulator complexes and disrupting their ability to form a chromatin domain.

caused subtle defects in insulator activity in a wild-type *mod(mdg4)* background (data not shown).

We performed epistasis analysis to obtain mechanistic insight into opposing effects on insulator function displayed by Argonaute and *Rm62* mutants. One possibility is that mutation of *piwi* or *aub* could inactivate the RNAi pathway and thereby increase the availability of Rm62 to reduce insulator function in an RNAi-independent manner. Combination of Argonaute and *Rm62* mutations would therefore be expected to show the same phenotype as *Rm62* mutants alone. However, we did not observe this outcome. Triple aub^{QC42}/+; $Rm62^E mod(mdg4)^{u1}$/$Rm62^{sh(3)029}$ $mod(mdg4)^{u1}$ and $piwi^2$/+; $Rm62^E mod(mdg4)^{u1}$/$Rm62^{sh(3)029}$$mod(mdg4)^{u1}$ flies showed the same effects on y^2 and ct^6 as double aub^{QC42}/+; $mod(mdg4)^{u1}$ and $piwi^2$/+; $mod(mdg4)^{u1}$ mutants, respectively (**Fig. 2b**). The epistasis results suggest that these genes affect insulator activity through a common RNAi-dependent pathway and further show that *piwi* and *aub* act upstream of *Rm62* with respect to insulator function.

Additional evidence suggests that altered insulator function in RNAi mutants is unlikely to be due to indirect effects. To rule out that Argonaute mutations decrease silencing of y^2 and ct^6, we examined the effect of *piwi* and *aub* mutations on omb^{P1-D11}, in which a *gypsy* insulator protects a *white* transgene from the repressive effects of *omb* regulatory elements[16]. In $mod(mdg4)^{T6}$ loss-of-function point mutants with defective insulator function, *white* expression is repressed in the midline of the eye (**Fig. 2c**)[6]. Combination of either $piwi^2$/+ or aub^{QC42}/+ with $mod(mdg4)^{T6}$ resulted in a further increase of *white* repression, confirming that insulator function is reduced. Next, protein blot analysis showed that CP190 and Su(Hw) insulator protein levels remained unchanged in $piwi^2$/+, aub^{QC42}/+, aub^{AP-3a}/+, and $Rm62^E$/$Rm62^{sh(3)029}$ mutants in the $mod(mdg4)^{u1}$ genetic background, indicating that effects on insulator function are not caused by altered expression of insulator component genes (**Fig. 2d**). However, RNAi mutants could affect expression of other genes that influence insulator activity. Finally, we examined the effect of *loquacious*, which encodes the protein partner of the enzyme Dicer-1 involved primarily in microRNA processing[19,20]. We did not observe any effects on y^2 or ct^6 in loq^{f00791}; $mod(mdg4)^{u1}$ compared with $mod(mdg4)^{u1}$ flies, suggesting that the microRNA pathway does not directly or indirectly influence insulator function (data not shown).

We compared the genome-wide localization of RNAi machinery and insulator proteins to address how RNAi affects insulator function. For *S. pombe* centromeric silencing, the RNAi machinery associates with the site of dsRNA transcription to recruit heterochromatin proteins[21]. We localized transgene-encoded myc-Piwi to highly replicated ovarian nurse cell polytene chromosomes. Driven by the endogenous *piwi* promoter, *myc-Piwi* expression shows restricted tissue specificity[22]. We observed extensive colocalization between the signal from antibodies to myc ((α-myc) and DAPI staining, indicating that myc-Piwi localizes to condensed regions of DNA (**Fig. 3a**). We detected a similar localization pattern for GFP-Aub overexpressed in salivary gland polytene chromosomes, and GFP-Aub was also present at the chromocenter, the site of centromeric heterochromatin (data not shown). GFP-Aub and myc-Piwi localization patterns were consistent with their roles in centromeric heterochromatin silencing and possibly throughout the genome[23]. In contrast, the localization patterns of Mod(mdg4)2.2 and Su(Hw) were distinct from that of GFP-Aub and myc-Piwi, with minimal staining at the chromocenter (**Fig. 3** and data not shown).

Unlike Argonautes, Rm62 localizes primarily to highly transcribed sequences. Rm62 associated predominantly with a small subset of interbands and ecdysone puffs, resulting from decondensation of genes highly transcribed during larval development (**Fig. 3b**). In addition, Rm62 localized to the chromocenter, consistent with its effect on heterochromatic silencing[13]. The differential localization patterns of Argonaute proteins and Rm62 in euchromatin may reflect roles for Rm62 in cellular mechanisms in addition to RNAi, such as RNA transport and transcription[24]. Comparison of localization patterns of Rm62 and CP190, which binds to hundreds of euchromatic sites, showed a limited degree of overlap, suggesting that these proteins interact transiently or outside the context of polytenized chromosomes (**Fig. 3b**). Rm62 and CP190 may interact during earlier stages of development, such as in embryos, from which we purified insulator complexes.

We determined the localization of insulator proteins on polytene chromosomes of RNAi mutants in order to test whether the RNAi machinery recruits insulator proteins to chromatin. We did not detect any changes in Su(Hw), Mod(mdg4)2.2 or CP190 association with euchromatic arms in $piwi^1$/$piwi^2$, aub^{AP-3a} or $Rm62^{EY6795}$/$Rm62^{sh(3)029}$ mutants as compared with wild-type larvae (**Fig. 4** and data not shown). In these experiments, we analyzed more severe pupal lethal $Rm62^{EY6795}$/$Rm62^{sh(3)029}$ transheterozygous loss-of-function mutants. We obtained the same results in the $mod(mdg4)^{u1}$ background (data not shown). Furthermore, insulator proteins remain associated with y^2, a *gypsy* insertion site (**Supplementary Fig. 1** online). These results and the finding that Argonautes, Rm62 and insulator proteins all show distinct patterns of genomic localization suggest that the RNAi machinery does not target insulator proteins directly to their genomic binding sites.

Conversely, mutation of the RNAi machinery alters the higher-order organization of insulator complexes. In wild-type larvae, CP190 localized to large nuclear foci in diploid imaginal disc and brain cells (**Fig. 5a**)[6]. However, in $mod(mdg4)^{u1}$ mutants, insulator body formation was disrupted, resulting in diffuse punctate nuclear localization of

CP190 (**Fig. 5a**)[9]. Notably, combination of $Rm62^E/Rm62^{sh(3)029}$ with $mod(mdg4)^{u1}$ restored insulator body localization to a wild-type pattern (**Fig. 5a**). Similarly, $CP190^{4-1}/CP190^{P11}$ mutants, which produce nonfunctional CP190 that does not concentrate in nuclear foci, showed defective insulator body formation with diffuse nuclear localization of Mod(mdg4), compared with wild-type larvae (**Fig. 5b**). $Rm62^E$ $CP190^{P11}/Rm62^{sh(3)029}$ $CP190^{4-1}$ double mutants showed partial restoration of Mod(mdg4) punctate nuclear staining (**Fig. 5b**). In contrast, $piwi^1/piwi^2;mod(mdg4)^{u1}$ and $aub^{QC42}/aub^{\Delta P-3a}$; $mod(mdg4)^{u1}$ double mutants showed more diffuse nuclear CP190 staining than $mod(mdg4)^{u1}$ mutants (**Fig. 5c**). The negative effects of Argonaute mutants and positive effects of $Rm62$ mutants on insulator body formation are consistent with their disruptive and beneficial effects, respectively, on insulator function (**Fig. 2a,b**). Moreover, Rm62 localized throughout nuclei of wild-type imaginal disc cells, overlapping with CP190 but not concentrated in nuclear foci (**Supplementary Fig. 2** online). These results suggest that Argonaute proteins contribute to higher-order insulator complex formation and that Rm62 negatively affects insulator function by hindering its ability to produce these structures.

Taken together, our results suggest the existence of an RNA species required for the formation or integrity of insulator bodies, perhaps a product of processing by Argonautes and the other RNAi machinery (**Fig. 6**). The putative RNA helicase Rm62 may be recruited to insulator complexes through physical interaction with CP190 and RNA. Although it is unknown at what mechanistic step Rm62 acts in RNAi, Rm62 may act downstream of Argonautes to unwind or remodel RNA-insulator protein complexes, thereby disrupting *gypsy* insulator activity and nuclear organization. Proper insulator body localization requires an intact nuclear matrix[9,10], and early observations identified RNA as an important component of this nuclear scaffold[25]. Future studies should determine the identity of putative *gypsy* insulator associated RNAs. Our results suggest a previously unknown function of the RNAi machinery in the control of nuclear architecture to effect changes in gene expression.

METHODS

Immunoaffinity purification of α-CP190 complexes. Embryos 3–18 h old were harvested from wild-type Oregon R flies raised at 22–25 °C in population cages and fed yeast and molasses. Embryos were dechorionated with 50% bleach, washed with water and stored at −80 °C until use. Forty grams of frozen embryos were ground in liquid nitrogen with a mortar and pestle, and nuclei were prepared as described[26]. All subsequent steps were performed at 4 °C. Nuclei were sonicated eight times for 10 s at 20 W in 5 ml PBSMT-0.3% (PBS, 3 mM MgCl₂, 0.3% Triton X-100 (vol/vol)) and spun down at 16,000g in a microcentrifuge. Soluble material was bound to Protein A Sepharose cross-linked covalently[27] to preimmune sera for 1 h and then bound to Protein A Sepharose cross-linked covalently to affinity-purified rabbit α-CP190 (ref. 6) for 1 h. Beads were washed three times with 15 ml of PBSMT-0.3% and once with 15 ml PBSM (PBS, 3 mM MgCl₂) and packed into a column by gravity. Sequential elutions using 1.3 ml of PBSM, with MgCl₂ concentrations as described, were collected and subjected to trichloroacetic acid precipitation. Samples were resuspended in denaturing sample buffer, separated on 4–12% SDS-PAGE, and protein blotted or stained with Coomassie blue. Bands of interest were subjected to in-gel trypsin digestion and matrix-assisted laser desorption/ionization–time of flight (MALDI-TOF) mass spectrometry at the Dana-Farber Cancer Institute Molecular Biology Core Facility (Boston). For RNase A treatment, nuclear extracts were incubated for 30 min with α-CP190–cross-linked Protein A beads before addition of 50 μg/ml RNase A for 30 min.

Fly strains. Flies were raised on standard medium at room temperature or 25 °C. Flies for immunostaining of ovarian nurse cells were raised at 18 °C. Larvae for immunostaining of imaginal disc and brain cells were raised at 25 °C. Larvae for immunostaining of polytene chromosomes were raised at 18 °C.

Antibody production. Recombinant N-terminal His-tagged fusion protein of the unique N-terminal (amino acids 10–166) and C-terminal ends (amino acids 488–578) of Rm62 (CG10279-PF) was purified from *E. coli* on a nickel-agarose column and used to immunize rats and rabbits using standard procedures.

Protein blotting. Protein lysates from third instar larvae were prepared as described previously[9]. Rat α-Su(Hw)[7] was used at a 1:5,000 dilution, rabbit α-CP190 at 1:10,000, rat α-Mod(mdg4)2.2 (ref. 28) at 1:5,000 and mouse α-p68 (ref. 12) (gift of F. Fuller-Pace, University of Dundee) at 1:3.

Immunofluorescence. Polytene chromosomes from otu^7/otu^{11} ovarian nurse cells were prepared essentially as described in ref. 29. Briefly, adult ovaries were dissected in PBS, stripped of mature eggs, fixed in a 3:2:1 ratio of acetic acid/water/lactic acid for 2 min and then squashed. Single chromosome arms were analyzed because of the fragility of chromosome spreads from this tissue. Staining with antibodies to myc was compared with chromosomes lacking the transgene. Preparation and immunostaining of salivary gland polytene chromosomes and imaginal disc and brain cells was performed as described previously[8]. Ecdysone puffs were marked by antibodies to Pep[30]. Rabbit α-CP190 was used at 1:400, rat α-CP190 (ref. 6) at 1:100, rat α-Su(Hw) at 1:100, rabbit α-Su(Hw) at 1:100 (ref. 7), rabbit α-Mod(mdg4)[7] at 1:100, rat α-Mod(mdg4)2.2 at 1:100, rat α-Rm62 at 1:20, rabbit α-GFP (TP401, Torrey Pines Biolabs) at 1:200, and rabbit α-myc (A14, Santa Cruz) at 1:10.

Note: Supplementary information is available on the Nature Genetics website.

1. Volpe, T.A. *et al.* Regulation of heterochromatic silencing and histone H3 lysine-9 methylation by RNAi. *Science* **297**, 1833–1837 (2002).
2. Pal-Bhadra, M. *et al.* Heterochromatic silencing and HP1 localization in *Drosophila* are dependent on the RNAi machinery. *Science* **303**, 669–672 (2004).
3. Hall, I.M., Noma, K. & Grewal, S.I. RNA interference machinery regulates chromosome dynamics during mitosis and meiosis in fission yeast. *Proc. Natl. Acad. Sci. USA* **100**, 193–198 (2003).
4. Grimaud, C. *et al.* RNAi components are required for nuclear clustering of Polycomb group response elements. *Cell* **124**, 957–971 (2006).
5. Parkhurst, S.M. *et al.* The *Drosophila* su(Hw) gene, which controls the phenotypic effect of the gypsy transposable element, encodes a putative DNA-binding protein. *Genes Dev.* **2**, 1205–1215 (1988).
6. Pai, C.Y., Lei, E.P., Ghosh, D. & Corces, V.G. The centrosomal protein CP190 is a component of the gypsy chromatin insulator. *Mol. Cell* **16**, 737–748 (2004).
7. Gerasimova, T.I., Gdula, D.A., Gerasimov, D.V., Simonova, O. & Corces, V.G. A *Drosophila* protein that imparts directionality on a chromatin insulator is an enhancer of position-effect variegation. *Cell* **82**, 587–597 (1995).
8. Gerasimova, T.I., Byrd, K. & Corces, V.G. A chromatin insulator determines the nuclear localization of DNA. *Mol. Cell* **6**, 1025–1035 (2000).
9. Capelson, M. & Corces, V.G. The ubiquitin ligase dTopors directs the nuclear organization of a chromatin insulator. *Mol. Cell* **20**, 105–116 (2005).
10. Byrd, K. & Corces, V.G. Visualization of chromatin domains created by the gypsy insulator of *Drosophila*. *J. Cell Biol.* **162**, 565–574 (2003).
11. Yusufzai, T.M. & Felsenfeld, G. The 5′-HS4 chicken beta-globin insulator is a CTCF-dependent nuclear matrix-associated element. *Proc. Natl. Acad. Sci. USA* **101**, 8620–8624 (2004).
12. Ishizuka, A., Siomi, M.C. & Siomi, H. A *Drosophila* fragile X protein interacts with components of RNAi and ribosomal proteins. *Genes Dev.* **16**, 2497–2508 (2002).
13. Csink, A.K., Linsk, R. & Birchler, J.A. The Lighten up (Lip) gene of *Drosophila melanogaster*, a modifier of retroelement expression, position effect variegation and white locus insertion alleles. *Genetics* **138**, 153–163 (1994).

14. Parkhurst, S.M. & Corces, V.G. Interactions among the gypsy transposable element and the yellow and the suppressor of hairy-wing loci in *Drosophila melanogaster*. *Mol. Cell. Biol.* **6**, 47–53 (1986).

15. Jack, J.W. Molecular organization of the cut locus of *Drosophila melanogaster*. *Cell* **42**, 869–876 (1985).

16. Tsai, S.F. *et al.* Gypsy retrotransposon as a tool for the in vivo analysis of the regulatory region of the optomotor-blind gene in *Drosophila*. *Proc. Natl. Acad. Sci. USA* **94**, 3837–3841 (1997).

17. Schupbach, T. & Wieschaus, E. Female sterile mutations on the second chromosome of *Drosophila melanogaster*. II. Mutations blocking oogenesis or altering egg morphology. *Genetics* **129**, 1119–1136 (1991).

18. Lin, H. & Spradling, A.C. A novel group of pumilio mutations affects the asymmetric division of germline stem cells in the *Drosophila* ovary. *Development* **124**, 2463–2476 (1997).

19. Forstemann, K. *et al.* Normal microRNA maturation and germ-line stem cell maintenance requires Loquacious, a double-stranded RNA-binding domain protein. *PLoS Biol.* **3**, e236 (2005).

20. Saito, K., Ishizuka, A., Siomi, H. & Siomi, M.C. Processing of pre-microRNAs by the Dicer-1-Loquacious complex in *Drosophila* cells. *PLoS Biol.* **3**, e235 (2005).

21. Noma, K. *et al.* RITS acts in cis to promote RNA interference-mediated transcriptional and post-transcriptional silencing. *Nat. Genet.* **36**, 1174–1180 (2004).

22. Cox, D.N., Chao, A. & Lin, H. piwi encodes a nucleoplasmic factor whose activity modulates the number and division rate of germline stem cells. *Development* **127**, 503–514 (2000).

23. Pal-Bhadra, M., Bhadra, U. & Birchler, J.A. RNAi related mechanisms affect both transcriptional and posttranscriptional transgene silencing in *Drosophila*. *Mol. Cell* **9**, 315–327 (2002).

24. Buszczak, M. & Spradling, A.C. The *Drosophila* P68 RNA helicase regulates transcriptional deactivation by promoting RNA release from chromatin. *Genes Dev.* **20**, 977–989 (2006).

25. Fey, E.G., Krochmalnic, G. & Penman, S. The nonchromatin substructures of the nucleus: the ribonucleoprotein (RNP)-containing and RNP-depleted matrices analyzed by sequential fractionation and resinless section electron microscopy. *J. Cell Biol.* **102**, 1654–1665 (1986).

26. Shaffer, C.D., Wuller, J.M. & Elgin, S.C.R. *Methods in Cell Biology* (Academic, San Diego, 1994).

27. Harlow, E. & Lane, D. *Antibodies: A Laboratory Manual* (Cold Spring Harbor Laboratory, New York, 1988).

28. Mongelard, F., Labrador, M., Baxter, E.M., Gerasimova, T.I. & Corces, V.G. Trans-splicing as a novel mechanism to explain interallelic complementation in *Drosophila*. *Genetics* **160**, 1481–1487 (2002).

29. Mal'ceva, N.I., Belyaeva, E.S., King, R.C. & Zhimulev, I.F. Nurse cell polytene chromosomes of *Drosophila melanogaster* otu mutants: morphological changes accompanying interallelic complementation and position effect variegation. *Dev. Genet.* **20**, 163–174 (1997).

30. Amero, S.A., Elgin, S.C. & Beyer, A.L. A unique zinc finger protein is associated preferentially with active ecdysone-responsive loci in *Drosophila*. *Genes Dev.* **5**, 188–200 (1991).